# A Novel Clutter Covariance Matrix Estimation Method Based on Feature Subspace for Space-Based Early Warning Radar

Tianfu Zhang, *Student Member, IEEE*, Zhihao Wang, *Student Member, IEEE*, Ning Qiao, Shuangxi Zhang, *Member, IEEE*, Mengdao Xing, *Fellow, IEEE*, and Yongliang Wang

***Abstract*—Accurate estimation of the clutter covariance matrix for the cell under test (CUT) is a committed step in the spatial-temporal adaptive processing (STAP) algorithm. The unique nonstationary characteristic of signal for space-based early warning radar (SBEWR) leads to the spatial variation of training sample and the insufficient number of optional independent identically distributed (i.i.d.) training samples, which brings difficulties to training sample selection and covariance matrix estimation. To improve the estimation accuracy of clutter covariance matrix and the performance of STAP for SBEWR in a heterogeneous environment, a novel training sample selection and clutter covariance matrix estimation method is proposed. The method based on clutter subspace reconstruction and spectrum correction technology can improve the estimation accuracy of clutter covariance matrix in the case of nonstationary signals and heterogeneous environments. The clutter covariance matrix estimated by the proposed method is similar to the clutter covariance matrix of the CUT, and the performance of STAP is improved. The experimental results confirm the performance of the proposed method.**

***Index Terms*—Covariance matrix estimation, heterogeneous environment, space-based early warning radar (SBEWR), spatial-temporal adaptive processing (STAP), training sample.**

## I. Introduction

SPATIAL-TEMPORAL adaptive processing (STAP) technology greatly improves the detect moving targets capability of radar in strong clutter and interference environments [1]–[3]. With the development of technology, the CFAR algorithm for target detection is becoming more and more mature, and various high accuracy CFAR detectors are proposed [4]–[7]. In order to use these CFAR detectors to accurately detect moving target information in the radar output power spectrum, it is necessary to suppress clutter and make the clutter spectrum clearer. In actuality, the clutter covariance matrix of the cell under test (CUT) is unknown, and the maximum likelihood estimation method is usually used to estimate the clutter covariance matrix [8]. The selection of training samples directly affects the estimation accuracy of the clutter covariance matrix. Inaccurate estimation of the clutter covariance matrix of CUT may result in insufficient clutter suppression and target signal cancellation [9]–[11]. To ensure the accuracy of clutter covariance matrix estimation, according to the R.M.B. criterion, when the maximum likelihood estimation method is used to estimate the clutter covariance matrix of CUT, at least two times the number of i.i.d. training samples are required [12], [13].

Compared with the traditional airborne early warning radar (AEWR), the working mode of SBEWR is beam-to-earth overlooking, and the ground clutter enters the range of the beam main lobe, which has a significant impact on the monitoring work. Moreover, the SBEWR has broader beam main lobe coverage, and the inhomogeneous ground clutter background is more complicated [14]–[15]. Due to its unique geometrical relationship between the satellite and the earth, the nonstationary factors brought by the earth's rotation and range ambiguity also make the working background of the SBEWR more complex [16]–[18], and these factors bring more difficulties to the selection of independent identically distributed (i.i.d.) training samples. The covariance matrix calculated directly from received data cannot completely construct the clutter subspace, so it cannot be directly applied to the calculation of adaptive weights in STAP.

In order to improve the performance of STAP in a nonhomogeneous environment, a series of algorithms have been proposed. Aiming at the problem of insufficient training samples, many STAP methods based on JDL or GMB are proposed [19], [20]. These methods use fixed dimension reduction structure to reduce the degree of freedom of clutter by local dimension reduction of clutter, which reduces the requirements of training samples for covariance matrix estimation. However, since the nonstationary characteristics of the echo are not considered, the nonstationary

Manuscript received September 26, 2021; revised October 14, 2021; accepted October 23, 2021. Date of publication October 29, 2021; date of current version November 15, 2021. This work is supported by the National Science Fund for Distinguished Young Scholars under Grant 61825105, the National Natural Science Foundation of China under Grant 61801387. *(Corresponding author: Shuangxi Zhang.)*

Tianfu Zhang and Zhihao Wang are with the National Laboratory of Radar Signal Processing, Xidian University, Xi'an 710071, China (e-mail: tianfuxdu@foxmail.com; ynwaamaranth@gmail.com).

Ning Qiao is with the School of Electronics and Information, Northwestern Polytechnical University, Northwestern Polytechnical University School of Electronics and Information, Xi'an, Shaanxi 710072, China (e-mail: qning@mail.nwpu.edu.cn).

Shuangxi Zhang is with the School of Electronics and information, Northwestern Polytechnical University, Xi'an 710072, China (e-mail: shuangxizhang1984@163.com).

Mengdao Xing is with the National Laboratory of Radar Signal Processing, Xidian University, Xi'an, Shaanxi 710071, China (e-mail: xmd@xidian.edu.cn).

Yongliang Wang is with the Department 3, Wuhan Radar Academy, Wuhan 430014, China (e-mail: ylwangkjld@163.com).

Digital Object Identifier 10.1109/JSTARS.2021.3123648

factors of the echo make it difficult for the local clutter dimension reduction method to completely suppress the clutter information in heterogeneous environments such as complex terrain and strong discrete scattering points. These reduced-dimensional STAP methods are more suitable for AEWRs with nonstationary characteristics, less range ambiguity. For SBEWR, even if these methods can accurately select qualified training samples, clutter suppression performance will decrease due to nonstationary factors. In addition, it is difficult to obtain complete clutter distribution characteristics by using these local clutter dimension reduction methods, which brings difficulties to the spatial variability compensation of clutter position information. A series of algorithms such as generalized inner product algorithm (GIP) and power selection training (PST) are proposed to solve the problem of selecting i.i.d. training samples in heterogeneous environments. The GIP algorithm selects samples by comparing the similarity degree of data structure between the training sample and the CUT. In the case that the CUT is nonindependent and identical with a large number of training samples, the training cell selected by the GIP algorithm cannot accurately estimate the clutter covariance matrix, and when there is no obvious strong interference target in the training cells, the estimation result of GIP method is inaccurate [21]–[24]. The characteristics of power spectrum broadening and spatial-temporal position spatial variation of SBEWR receiving echo also make the basic PST algorithm no longer applicable [25]. These two traditional sample selection methods cannot cope with the unique nonstationary environment of SBEWR, even after reducing the number of training samples, these methods can well select the training samples that meet the i.i.d. conditions. The covariance matrix estimated by these training samples will also significantly reduce the clutter suppression performance. In addition, a series of knowledge-aided methods are proposed to select training samples [26], [27], those knowledge-aided methods can select the training samples whose clutter amplitude satisfies the i.i.d. condition, and the problem of sample space variability caused by nonstationary factors cannot be solved in those methods.

In this article, a training sample selection and clutter covariance matrix estimation method that can be applied to the working environment of SBEWR is proposed. The clutter information contained in the training samples is analyzed, and the clutter information can be divided into clutter amplitude information and clutter position information. Based on the fitting degree between the eigenvalue spectrum of the covariance matrix of the training sample and the CUT, a series of training samples meeting i.i.d. conditions are selected in the heterogeneous environment, and then the clutter position information of each selected training sample is corrected to estimate the clutter covariance matrix of CUT. This proposed method can make up for the shortcomings of traditional methods in the nonstationary and heterogeneous environment, and greatly improves the clutter suppression and moving target detection performance of SBEWR in a heterogeneous environment.

The rest of this article is outlined as follows. The geometric model and received signal model of SBEWR are in Section II. In Section III, the clutter subspace reconstruction is proposed, which is used to restore the clutter information contained in the training samples. Moreover, the training samples are selected according to the similarities, and the spatial variability of clutter position information is corrected. Section IV illustrates the experimental results and analysis of the performance. Finally, Section V concludes the article.

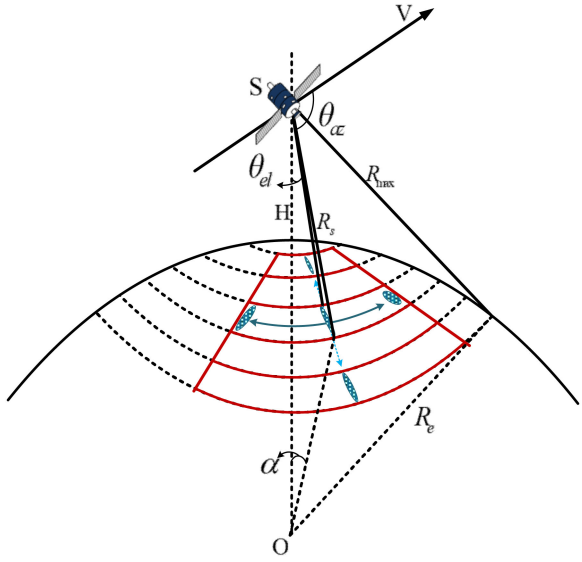


Fig. 1. Geometric model of SBEWR.

## II. Model

The main lobe of the antenna beam is completely covered on the earth's surface when the SBEWR is in the working mode of monitoring moving targets in the near space. The observation geometric model of SBEWR is shown in Fig. 1.

$O$is the center of the earth, $S$is the SBEWR, vector $V$ represents the speed direction of the satellite, the height of orbit is expressed by $H$, and the earth radius is $R_e$.$\theta_{az}$ and$\theta_{el}$are the azimuth and elevation angles of the antenna transmitting beam, respectively. Due to the limitation of earth curvature, the farthest operating distance of space-based early warning radar (SBEWR) is $R_{\max}$.To meet early warning requirements for specific region, the search mode based on the fixed beam direction cannot satisfy the detection of the whole interested area, therefore, it is necessary to achieve flexible beam control by an active phased array antenna. The scanning of the antenna beam is divided into two dimensions of pitch and azimuth to complete the scanning and tracking of the target in the whole early warning region.

In Fig. 1, the geocentric angle of the beam is represented by $\alpha$

$$\alpha = \arcsin\left(\frac{R_e + H}{R_e}\sin\theta_{\mathrm{el}}\right) - \theta_{\mathrm{el}}. \tag{1}$$

The relationship between the slant range along radar beam center $R_s$ and elevation angle $\theta_{\mathrm{el}}$ can be expressed as

$$\theta_{\mathrm{el}} = \arccos\left(\frac{H^2 + 2R_eH + R_s^2}{2\left(H + R_e\right)R_s}\right). \tag{2}$$

The number of range ambiguity in the main lobe of SBEWR is determined by the antenna size and the pulse repetition frequency (PRF) of the radar system, and the unambiguous range can be expressed by $r_u = c/2f_r$. Because the radar is in low earth orbit, the main lobe of elevation dimension of SBEWR covers a wide range, and the range ambiguity effect is obvious. Besides due to the rotation of the earth, the received data of different range ambiguity positions deviates in the spectrum. These factors lead to the broadening of the clutter power spectrum and introduce the spatial variability of spatial-temporal spectrum in the distance dimension, which brings difficulties to the estimation of the clutter covariance matrix.

The distance of each range ambiguity position can be expressed as $R_{s_i} = R_s + ir_u$, where $i$ is the range ambiguity number of this position. The elevation angles corresponding to different range ambiguity positions are calculated by (2).

In practice, due to the limitation of antenna feed, in order to reduce the amount of calculation in the adaptive algorithm and improve the real time performance of the system. The multichannel signal processing method is used to reduce the dimension of the received data [29], [30]. The transmitting array uses the array element level fixed beamforming, and the receiving array uses the multichannel subarray division form for adaptive beamforming. The antenna is a linear array containing $N$ elements, and the element spacing $d$ is half of the signal wavelength. One CPI contains $K$ pulses. The data received by each array element is

$$\mathbf{x} = \sigma \mathbf{s}\left(\omega_d, \psi\right) = \sigma \mathbf{s}_t\left(\omega_d\right) \otimes \mathbf{s}_s\left(\psi\right). \tag{3}$$

$\mathbf{s}$is spatial-temporal steering vector

$$\begin{aligned} \mathbf{s}_t &= \left[1 e^{-j\pi\omega_d} e^{-j2\pi\omega_d} \cdots e^{-j(K-1)\pi\omega_d}\right]^T \\ \mathbf{s}_s &= \left[1 e^{-j\pi\cos\psi} e^{-j2\pi\cos\psi} \cdots e^{-j(N-1)\pi\cos\psi}\right]^T. \end{aligned} \tag{4}$$

Equation (4) is the time and space steering vectors, respectively. $\sigma$, $\psi$ and $\omega_d$ represent the amplitude of the received signal, the direction of arrival angle (DOA), and the Doppler frequency of the received signal. $\cos\psi = \sin\theta_{el}\cos\theta_{az}$, due to the Doppler frequency shift caused by earth rotation, the Doppler model of clutter cell is modified to $\omega_d = \frac{2VT_r}{\lambda}\rho_c \sin\theta_{el}\cos(\theta_{az} + \varphi_c)$ [16]. $\rho_c$ and $\varphi_c$ are the yaw amplitude and yaw angle caused by the earth rotation, respectively. $\lambda$ and $T_r$ are the frequency and the pulse repetition interval (PRI) of the system. The nonuniform subarray division form is used to avoid the grating lobe caused by subarray synthesis and improves the performance of clutter suppression. The linear array containing $N$ elements are divided into $M$ channels by matrix $D_M$ and the number of elements contained in each channel is$m_i, i = 1, 2 \cdots M$. Each channel does not contain the same array element when we design the partitioning strategy, $\sum_{i=1}^{M} m_i = N$

$$\mathbf{D}_M = \begin{bmatrix} \mathbf{I}_{m_1} & \mathbf{0} & \cdots & \mathbf{0} \\ \mathbf{0} & \mathbf{I}_{m_2} & \cdots & \mathbf{0} \\ \vdots & \vdots & \ddots & \vdots \\ \mathbf{0} & \mathbf{0} & \cdots & \mathbf{I}_{m_M} \end{bmatrix}_{N \times M}. \tag{5}$$

$\mathbf{I}_{q_i}$ represents a column vector with all elements of 1, and the length is $q_i$.The weighting of each array element is

$$\mathbf{T}_d = \mathbf{D}\left(w\right)\mathbf{D}\left(\theta\right)\mathbf{D}_M. \tag{6}$$

$\mathbf{D}(w)$ is the amplitude windowing of antenna elements, such as Chebyshev window, Taylor window, etc. $\mathbf{D}(\theta)$represents the beam direction of the array elements level antenna pattern. The spatial steering vector at the subarray level of the received signal is $\mathbf{s}_{s\_sub} = \mathbf{T}_d^H \mathbf{s}_s$, the spatial-temporal steering vector is $\mathbf{s}_{\text{sub}} = \mathbf{s}_t \otimes \mathbf{s}_{s\_\text{sub}}$. The covariance matrix of the received data at the array element is $\mathbf{R}$, and the covariance matrix of the data synthesized through the channel is expressed as

$$\mathbf{R}_{\text{sub}} = \mathbf{T}^H \mathbf{R} \mathbf{T}. \tag{7}$$

The dimension reduction matrix is

$$\mathbf{T} = \begin{bmatrix} \mathbf{T}_d & \mathbf{0} & & \mathbf{0} \\ \mathbf{0} & \mathbf{T}_d & & \\ & & \ddots & \mathbf{0} \\ \mathbf{0} & & \mathbf{0} & \mathbf{T}_d \end{bmatrix}_{NK \times MK}. \tag{8}$$

The adaptive weight vector is used as the weight of the second stage antenna pattern, that is, the weight of the channel data, can be expressed as

$$\mathbf{w}_{\text{sub}}\left(\omega_d, \psi\right) = \beta \mathbf{R}_{\text{sub}}^{-1} \mathbf{s}_{\text{sub}}\left(\omega_d, \psi\right). \tag{9}$$

## III. Covariance Matrix Estimation Method

### A. Clutter Subspace Reconstruction

According to Ward's clutter receiving model [28] and referring to the antenna parameters of SBEWR designed by the US Air Force and NASA [2]. The ground clutter receiving data is simulated by using the parameters giving in Table I. In a sample cell $l$, $N_c$ clutter patches are divided in azimuth direction according to the size of azimuth resolution, considering that the distance ambiguity is in the pitch dimension main lobe, the received data in a sample cell can be expressed as

$$\mathbf{x}_l = \sum_{j=1}^{N_r}\sum_{i=1}^{N_c} \sigma_{ij} \mathbf{s}\left(\omega_{d_{ij}}, \psi_{ij}\right) = \sum_{j=1}^{N_r}\sum_{i=1}^{N_c} \sigma_{ij} \mathbf{s}_t\left(\omega_{d_{ij}}\right) \otimes \mathbf{s}_s\left(\psi_{ij}\right) \tag{10}$$

where $N_r$ represents the distance ambiguity number contained in the main lobe of beam elevation dimension. $\sigma_{ij}$, $\psi_{ij}$ , and $\omega_{d_{ij}}$ are unknown, represents the received signal amplitude, DOA and corrected Doppler frequency of the received signal of the$i$ th clutter patch at the $j$ th range ambiguity position, respectively. The data of a sample cell received by radar is the superposition of the clutter patch data at all range ambiguity positions.

The covariance matrix of the data received by the sample cell $l$ is $\mathbf{R} = \mathbf{x}_l \mathbf{x}_l^H$, but it is inevitable to produce cross terms when the data between each clutter patch is accumulated and multiplied. These cross terms cause the covariance matrix of received data to be not an ideal Toeplitz matrix

$$\mathbf{R} \neq \sum_{j=1}^{N_a}\sum_{i=1}^{N_c} \sigma_{ij}^2 \mathbf{s}\left(\omega_{d_{ij}}, \psi_{ij}\right) \mathbf{s}^H\left(\omega_{d_{ij}}, \psi_{ij}\right). \tag{11}$$

TABLE I
SBEWR PARAMETERS

| Parameter | Symbol | Value |
|---|---|---|
| Orbit height | $H$ | 500km |
| Platform velocity | $V$ | 7600m/s |
| Center frequency | $f_c$ | 0.55GHz |
| PRF | $f_r$ | 5000Hz |
| Pulse number | $K$ | 32 |
| Bandwidth | $B$ | 0.8MHz |
| Array size | $D_a$ | 50m |
| | $D_r$ | 3m |
| Element number | $N$ | 183 |
| Spatial channel number | $M$ | 16 |
| Patch number | $N_c$ | 151 |
| Range ambiguity number | $N_r$ | 3 |
| Beam position | $\theta_{az}$ | 90° |
| | $\theta_{el}$ | 30° |

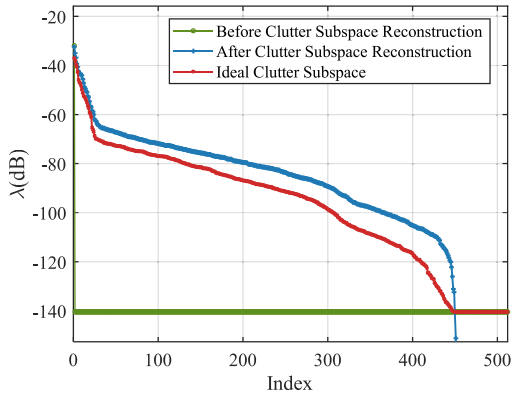


Fig. 2. Eigenvalue spectrum of clutter covariance matrix under different conditions.

Using the covariance matrix directly calculated by the received data will result in that the covariance matrix of the clutter cannot reflect the amplitude information of each clutter receive patch and the position information of the clutter receive patch on the spatial-temporal plane.

Computing eigenvalues and eigenvectors of the covariance matrix $\mathbf{R}$. Using a unitary matrix to represent covariance matrix $\mathbf{R}$, $\mathbf{R} = \mathbf{ULU}^H$, where, $\mathbf{L} = \mathrm{diag}([\lambda_1 \lambda_2 \cdots \lambda_{NK}])$ is a diagonal matrix composed of eigenvalues of covariance matrix. The result of eigenvalues spectrum obtained by different calculation methods of clutter covariance matrix are shown in Fig. 2, and the number of large eigenvalues of covariance matrix $\mathbf{R}$ is much less than the number of clutter patches, that is, the eigenvalues and eigenvectors of the covariance matrix cannot represent the amplitude and position information of the subspace corresponding to each clutter receive patch. These factors will lead to the fact that the adaptive weight $\mathbf{w}$ calculated by the covariance matrix $\mathbf{R}$ cannot accurately form a null value at the position of the clutter in the spatial-temporal plane.

The received clutter cells are divided based on the geometry model of SBEWR and Ward's clutter receive model. The pitch angle corresponding to the $j$th range ambiguity position of a receiving cell is $\theta_{el_j}$ and the azimuth angle of the $i$th receive patch is $\theta_{az_i}$.We can calculate the Doppler frequency corresponding to all clutter patches in a receive cell and all its corresponding range ambiguous positions based on the modified Doppler model. According to the location of each clutter patch obtained by the geometric model, we design a fixed spatial-temporal two-dimensional filter

$$\mathbf{w}_{ij} = \mathbf{s}\left(\omega_{d_{ij}}, \psi_{ij}\right) = \mathbf{s}_t\left(\omega_{d_{ij}}\right) \otimes \mathbf{s}_s\left(\psi_{ij}\right). \tag{12}$$

According to the clutter receiving unit divided by Ward's clutter receiving model, the spatial-temporal vector of each clutter receiving patch in several distance cells is calculated and stored in the form of a data matrix to form a spatial-temporal steering vector database. Due to the satellite flight is more stable than aircraft platforms, we can get the received signal amplitude for each clutter patch by using the designed spatial-temporal filter $\sigma_{ij} \approx \mathbf{w}_{ij}^H \mathbf{x}_l / NK$.

Finally, we can calculate a covariance matrix that contains all the clutter amplitude and position information, the covariance matrix of the all information of the receiving cell is constructed as

$$\mathbf{R}_{\mathrm{rc}} = \sum_{j=1}^{N_r} \sum_{i=1}^{N_c} \sigma_{ij}^2 \mathbf{s}\left(\omega_{d_{ij}}, \psi_{ij}\right) \mathbf{s}^H\left(\omega_{d_{ij}}, \psi_{ij}\right). \tag{13}$$

Compared with the covariance matrix directly calculated from the original received data, the reconstruction covariance matrix does not contain the cross-term information between different clutter patches. The additional eigenvectors and eigenvalues completely construct the signal subspace of received data. $\mathbf{R}_{\mathrm{rc}}$ is an ideal Toeplitz matrix. In this way, the whole clutter subspace information can be obtained by calculating the data of a single training sample. When the maximum likelihood method is used to estimate the clutter covariance matrix of the CUT, the rank of the estimated clutter covariance matrix is not limited to the number of samples.

The eigenvalues of the covariance matrix after the clutter subspace reconstruction are slightly higher than that in the ideal case, which is because the spatial-temporal two-dimensional filter has a certain width, resulting in the estimation error of the signal amplitude of the clutter patches. This error will reduce the clutter suppression performance, but will not affect the selection of training samples. The number of large eigenvalues contained in the reconstructed clutter covariance matrix is close to that in the ideal case. This shows that the reconstructed covariance matrix can represent all the support directions of the clutter subspace, including the amplitude and position information of all clutter receiving patches. Through the above discussion and the simulation analysis of eigenvalue spectrum, we can know that the covariance matrix of the clutter or the spatial-temporal power spectrum of the clutter contains two kinds of information. One is

the amplitude information of the clutter receiving patches, and the other is the position information of the patches in the spatial-temporal plane. In the processing of training sample selection, it is necessary to select the range cell with i.i.d. of the signal amplitude of the CUT. Therefore, it is more convenient to select suitable training samples by comparing amplitude information, which can improve the accuracy of clutter covariance matrix estimation.

Using the adaptive weight $\hat{\mathbf{w}} = \beta \hat{\mathbf{R}}_{rc}^{-1}\mathbf{s}$, calculated by the reconstructed clutter covariance matrix $\hat{\mathbf{R}}_{\mathrm{rc}}$, can obtain great clutter suppression performance. Otherwise, due to the incomplete construction of clutter space, the system cannot obtain ideal clutter suppression performance, and even cause cancellation of target signals.

### B. Covariance Spectrum of Heterogeneous Environment

In order to avoid canceling the target signal, the CUT cannot be used as the source of clutter information directly. The cells that meet the i.i.d. condition close to the CUT are selected as training samples, and the maximum likelihood estimation method is used to estimate the clutter covariance matrix of CUT.

In the working environment of SBEWR, according to the previous analysis, we can know that the nonstationary factors lead to the spatial variation of the clutter data of each training sample in the range direction. Moreover, due to the lack of the limitation of range ambiguity, in general, the number of training samples that can be selected cannot meet the R. M. B. criterion. The traditional sample selection method cannot be well applied to the spatial variation of clutter position between training samples. Therefore, the proposed method starts from the eigenvalue spectrum of clutter covariance matrix, and compares the amplitude information of clutter from different training samples, so as to avoid the influence of spatial variation of clutter position information on sample selection. According to Fig. 2, the number of large eigenvalues in eigenvalue spectrum is related to the number of clutter patches $N_c$, $N_r$. In general, a clutter patch corresponds to an eigenvalue in the eigenvalue spectrum and an eigenvector that forms the clutter subspace. The magnitude of eigenvalues is related to the signal amplitude of the corresponding clutter patch. The clutter subspace formed by the i.i.d. training samples of CUT is consistent with the clutter subspace of CUT. For training samples that do not completely satisfy i.i.d. conditions, the more similar the constructed clutter subspace, the more accurate the estimation of the clutter covariance matrix of CUT. The similarity of eigenvalue spectrum between different cells can be used as an evaluation index of similarity between cells.

In practice, the ground clutter environment of SBEWR is heterogeneous and complex. Table II classifies several representative terrains to describe the influence of special terrain on eigenvalue spectrum and STAP performance. In order to obtain accurate adaptive weight, ensure the depth and width of the filter notch and not cancel the target signal, it is necessary to design a training sample selection strategy suitable for most terrains.

TABLE II
HETEROGENEOUS TERRAIN EFFECTS

| Scene | Terrain Feature | Effect |
|---|---|---|
| *City and Town* | The particularity of urban buildings can cause abnormal change of clutter patches, which are regarded as interference patches. | The eigenvalue spectrum of a cell may have abnormal eigenvalues, resulting in false cancellation of the target signal. The cell can still be used as an alternative training sample after eliminating the abnormal eigenvalues. |
| *Mountain Land* | The clutter energy is high in this terrain. The variation of clutter amplitude is mainly caused by topography fluctuation. | Some unique ridges of the mountain will cause strong reflection points, and the elevation of terrain may also affect the amplitude distribution of eigenvalues, which will bring errors to the selection of training samples. |
| *Coastline* | The RCS of the ground scene at the land-sea interface changes rapidly. The amplitude distribution of different samples varies greatly, and the distribution range of eigenvalues of different training samples varies greatly. | The probability that the cells does not meet the i.i.d condition is large. It is easy to have problems such as insufficient depth and width of null notch in MDV performance curve and inaccurate location of notch. Eigenvalue spectrum of different cells are more easily distinguished. |
| *Sea* | The terrain is stable, and the amplitude of the received clutter is mainly modulated by the antenna pattern. Wind and waves can also affect the RCS distribution of the terrain. The eigenvalue distribution of different training samples is similar and the value is low. | Almost all cells can be used as training samples to estimate clutter covariance matrix. The difference between two cells mainly comes from sea surface waves. |

### C. Training Sample Selection Based on KL Divergence

In order to compare the eigenvalue spectrum between different training samples, the eigenvalue of the covariance matrix of each training sample data is calculated. The eigenvalue of the covariance matrix of CUT is represented by $\mathbf{r} = [\rho_1 \rho_2 \cdots \rho_{r_c}]$, and $\mathbf{l} = [\lambda_1 \lambda_2 \cdots \lambda_{r_c}]$ is the eigenvalue of training sample. Due to the large DOF of SBEWR systems and the heterogeneous terrain, alternative training sample resources are valuable. In order to ensure sufficient number of training samples, we need to take full advantage of each training sample. If the eigenvalue spectrum of training sample has very individual outliers compared with the neighboring cells, the abnormal eigenvalue is identified and eliminated through the offset Euclidean distance, and the training sample is still included in the alternative cell used to estimate the covariance matrix, rather than directly ignoring the cell. Second, when selecting training samples by comparing the similarity of eigenvalue spectrum, the weight of the interval where the larger eigenvalue is located should

be increased. Finally, the KL divergence (KLD) between the eigenvalues of different samples is calculated to evaluate the similarity between the samples [31]–[33].

We divide the distribution range of eigenvalues of covariance matrix into $N_e$ intervals. The size of each interval is

$$\Delta = \frac{\max\left([\rho_1 \rho_2 \cdots \rho_{r_c}]\right) - \min\left(([\rho_1 \rho_2 \cdots \rho_{r_c}])\right)}{N_c}. \quad (14)$$

Then, it is necessary to count the distribution probability of eigenvalues of the covariance matrix of CUT and each training sample in each interval and increasing the weights of distribution areas with large eigenvalues. The statistical results show that the probability density function of the eigenvalues of the covariance matrix of CUT and training sample is $P(\rho)$ and $Q(\lambda)$, eliminating the distribution interval with zero probability, the KLD between two cells can be calculated by (15)

$$\mathrm{KL}\left(Q \,\|P\right) = \sum_{\substack{i=1 \\ P(\rho_i)\neq 0}}^{N_e} Q\left(\lambda_i\right) \log_{10} \frac{Q\left(\lambda_i\right)}{P\left(\rho_i\right)}. \quad (15)$$

There is no eigenvalue in a distributed interval for training sample when $Q(\lambda)$ is zero. In this distribution area, $\mathrm{KL}(Q\|P)$ is zero, but this situation is obviously not conducive to estimation the covariance matrix of CUT. In order to avoid this situation, it is necessary to increase the penalty function when calculation KLD between the eigenvalues of CUT and training sample, and increase the weight of large eigenvalue interval. The modified KLD function is

$$\mathrm{KL}\left(Q \,\|P\right) = \sum_{\substack{i=1 \\ P(\rho_i)\neq 0}}^{N_e} WQ\left(\lambda_i\right) \log_{10} \frac{Q\left(\lambda_i\right)}{P\left(\rho_i\right)} + \sum_{\substack{P(\rho_i)\neq 0 \\ Q(\lambda_i)=0}}^{n} \frac{N_c - i}{\sigma_{\mathrm{penalty}}}. \quad (16)$$

The significance of penalty function is that when the eigenvalues of training samples do not exist in a certain interval of CUT's eigenvalues, the evaluation of similarity between them is reduced, and the larger the missing eigenvalue interval, the more obvious the effect. $W$ in the first term is the weight coefficient. Similarly, increasing the weight of the large eigenvalue interval and decreasing the weight of the small eigenvalue interval can improve the accuracy of training sample selection. The eigenvalues of CUT and training sample are most similar when the KLD of $P(\rho)$ and $Q(\lambda)$ is zero. We select samples with smaller KLD as training samples for estimating the covariance matrix of clutter. Compared with other algorithms, the training sample selection method based on eigenvalue spectrum can avoid the inversion of covariance matrix of each sample and reduce the requirement of system computing performance greatly.

### D. Training Sample Spatial Variation Correction

Compared with the traditional AEWR, the SBEWR platform moves faster and has a long operating distance. These factors lead to the spatial variability of the position distribution of the received clutter in the spatial-temporal plane in the different distance cells. Because the main lobe of the beam is completely covered on the earth surface, resulting in that the clutter distribution in the spatial-temporal plane is mainly the main lobe clutter, the spatial variability cannot be ignored. If we ignore the spatial variability of the position information and directly use the covariance matrix of the training sample to estimate the clutter information of the CUT, it will lead to the inaccurate estimation of the clutter covariance matrix of the CUT and the decrease of the clutter suppression performance. Therefore, before using the clutter information of training samples to estimate the clutter information of the CUT, it is necessary to correct the spatial variability of this position information [34], [35].

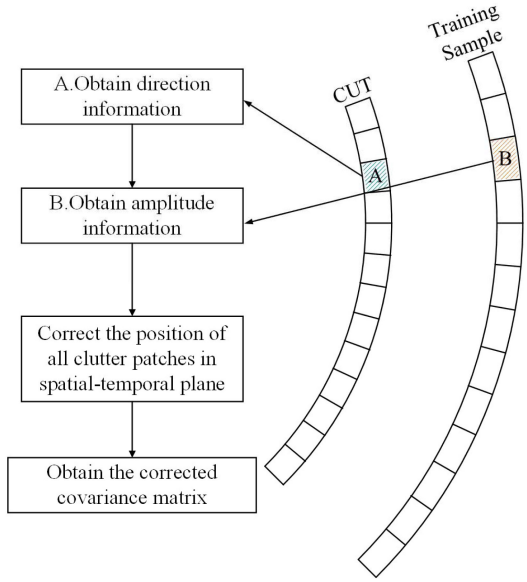


Fig. 3. Correction process of clutter position spatial variability training samples.

The correction process of spatial variability of training sample position information is as follows. First, the spatial-temporal steering vector of each clutter receiving patch in CUT in the steering vector library to determine the position information based on the CUT itself. The second step is to extract the amplitude information of each azimuth clutter receiving patch in selected training samples. In the third step, taking the clutter receiver patch in Fig. 3 as an example, the position information of patch A is fused with the amplitude information of patch B. Combined with two aspects of information, the covariance matrix of all clutter patches is calculated. The obtained training sample clutter covariance matrix is the covariance matrix that retains the amplitude information and eliminates the spatial deformation of spatial-temporal plane position.

Finally, Fig. 4 shows a flow diagram of clutter suppression for SBEWR. In order to prevent the effective target from being canceled in CUT, several cells adjacent to CUT are used as protection cells and are not used as training samples for clutter covariance matrix estimation. Then we extract the data of CUT and each cell, and reconstruction the clutter subspace of these data. Analyzing and comparing the eigenvalue spectrum of each

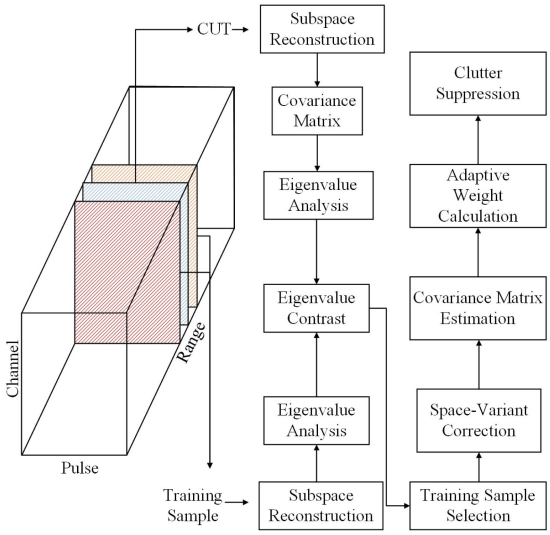


Fig. 4. Clutter covariance estimation process and clutter suppression process.

cell, selecting the cell whose eigenvalue spectrum is most similar to the CUT as the training sample for estimating the clutter covariance matrix. After the null variation correction of all the selected training samples, the maximum likelihood estimation method is used to estimate the clutter covariance matrix of the CUT. Finally, the estimate clutter covariance matrix is

$$\hat{\mathbf{R}} = \frac{1}{N_t}\sum_{i=1}^{N_t}\mathbf{R}_i. \tag{17}$$

The adaptive weight calculated with the estimate clutter covariance matrix is $\hat{\mathbf{w}}(\omega_d, \psi) = \beta\hat{\mathbf{R}}^{-1}\mathbf{s}(\omega_d, \psi)$.

## IV. Simulation

### A. Covariance Matrix Estimation Method Based on Random Terrain

In order to verify the accuracy of the proposed method through simulation, we set the clutter environment that conforms to different clutter fluctuation models, and the clutter fluctuation models satisfy Weibull distribution and logarithmic distribution, respectively. In addition, we set up three representative terrains, namely ocean, farmland, and mountains. Finally, we randomly distribute the above special terrains with different distributions in different range cells.

The Ward model is used to divide the receiving area of the ground clutter environment. The simulation of receiving data for SBEWR is based on the radar parameters set in Table I. According to $r_u = c/2f_r$, we can calculate the maximum unambiguous distance of the SBEWR is 30 km, and the maximum unambiguous distance contains 200 range sampling cells. All range cells are numbered according to the range resolution of the radar system, we set the elevation angle of the transmitting beam as 30°, and take the range bin numbered as 600 corresponding to the beam center as the CUT. Considering the unique influence of

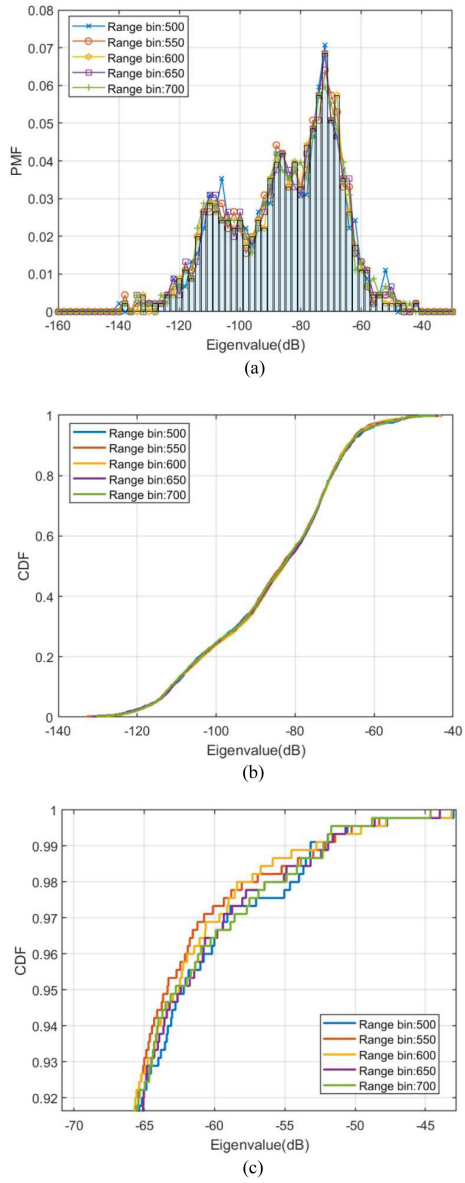


Fig. 5 (a) PMF of the eigenvalue (received clutter amplitude) of different samples. (b) CDF of the eigenvalue of different samples. (c) CDF of the eigenvalue [part of (b)].

nonstationary factors such as earth rotation and distance ambiguity of SBEWR, the range ambiguity number in the main lobe of the elevation dimension $N_r$ is three, including one forward ambiguity and one backward ambiguity. Moreover, due to the limitation of range ambiguity, the number of range cells available for training samples is 500–700.

According to the method proposed in Section III-A, after clutter subspace reconstruction of received clutter data for each range cell, we analyze eigenvalues of covariance matrix for each range cell data. Then we compare the similarity between the eigenvalue spectrum of each range cell and the eigenvalue spectrum of the CUT numbered 600. Taking the four range cells numbered 500, 550, 650, and 700 as an example, the PMF and CDF modeling of their eigenvalues are shown in Fig. 5. According to (16), the KL divergences between the

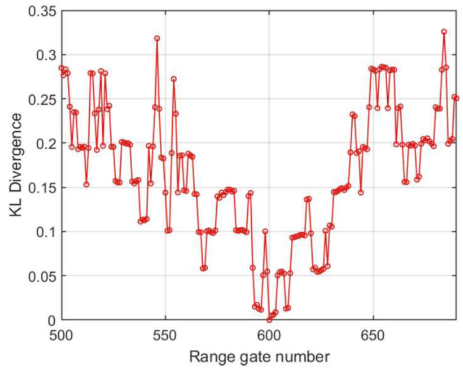


Fig. 6. KL divergence between CUT and each adjacent sample.

eigenvalue distributions are calculated to be 0.28, 0.14, 0.28, and 0.25, respectively. The KL divergence between CUT and each adjacent sample is shown in Fig. 6.

Next, we set the threshold and select samples with KL divergence lower than the threshold as training samples for estimating clutter covariance matrix.

In order to ensure the accuracy of clutter information estimation of the CUT, the method proposed in Section III-D is also needed to correct the position information of the data of each training sample in the spatial-temporal plane. We analyze the range bin numbered 500 as a training sample. The spatial-temporal Capon power spectrum is shown in Fig. 7(a) when the training sample is not corrected, and the spectrum of CUT is shown in Fig. 7(b), (d), and (e) represents the position distribution of each azimuth clutter patch in the training sample and CUT on the spatial-temporal plane. If the spatial variability is not correct, even if the selected training samples meet the criterion of i.i.d. with the CUT, in the process of estimation clutter covariance matrix, the spatial-temporal distribution of clutter patches in all training samples is not uniform, which leads to the serious broadening of the clutter power spectrum in the spatial and temporal dimensions, resulting in the widening of MDV curve concave and serious decline of clutter suppression performance. The proposed method is used to correct the clutter position information in the training sample, as shown in Fig. 7(f). The position of the clutter patches of the training sample are moved, so that the clutter position information of the training sample is consistent with the information of the CUT, and the spatial variability of the clutter position is eliminated. Using the corrected data to calculate the clutter power spectrum, and the result is shown in Fig. 7(c). The spatial-variant correction is carried out for each select training sample, and then the corrected data are used to estimate the clutter covariance matrix. The clutter information contained in the estimated covariance matrix will not be broadened in both spatial and temporal dimensions. The proposed correction method can greatly reduce the width of the concave of the MDV curve and improved the detection performance of the system.

Finally, the MDV performance of the system under different conditions is shown in Fig. 8. To evaluate the clutter suppression performance of different algorithms, the SCNR loss of the system $L_{\mathrm{SINR}}$ can be expressed as

$$L_{\mathrm{SINR}} = \frac{\mathrm{SINR}_{o\_nc}}{\mathrm{SINR}_{o\_n}} = \frac{S^H R_{\mathrm{cn}}^{-1} S}{S^H R_n^{-1} S}. \tag{18}$$

Case 1: The theoretical optimal clutter suppression performance of the system can be obtained by using the full space-time adaptive calculation of the array element level, in which the clutter covariance matrix uses the simulation value, $\mathbf{R}_c = \sum_{j=1}^{N_r} \sum_{i=1}^{N_c} \mathbf{x}_{ij}^H \mathbf{x}_{ij}$.

In practice, due to the large amount of data in the array element level, whether it is read and write or operation, all factors bring difficulties to the calculation system. For receiving data, channel synthesis is generally carried out first, and then data reading and writing and subsequent operation are carried out. The following simulation experiments are also based on channel dimension data.

Case 2: The traditional method first uses the JDL clutter dimension reduction method to reduce the estimation covariance matrix, according to the R.M.B. criterion, reduced the number of the required training samples. Then, the GIP method is used to select the training samples. Finally, the maximum likelihood estimation method is used to obtain the clutter covariance matrix $\hat{\mathbf{R}}_{n\_\mathrm{JDL}}$.

Case 3: The proposed method is used to process the data of each range cell. After the selection of training samples and the spatial correction of the selected samples, the estimated clutter covariance matrix is obtained $\hat{\mathbf{R}}_{n\_\mathrm{proposed}}$.

Case 4: The GMB method is used to reduce the dimension of the received clutter, and then the GIP method is used to select the training samples, and the estimated clutter covariance matrix $\hat{\mathbf{R}}_{n\_\mathrm{GMB}}$ is used for clutter suppression.

### *B. Clutter Suppression Performance Analysis of Algorithm Based on Real Terrain*

To simulate the performance of the proposed method in real ground clutter scenes, we use the surface image obtained by SAR satellite GF-3 as the simulated terrain environment data to simulate the proposed method. The terrain of the clutter environment is shown in Fig. 9, where different colors represent different land types. The blue area is the ocean, the red area is artificial buildings with high RCS value, and the yellow-green area represents the hilly, farmland, mountainous, and other fields with low RCS values. The grazing angle of the beam relative to each clutter block is calculated through the geometric relationship, which is substituted into the Morchin model of the ground-sea clutter to obtain the RCS value of the clutter receiving patch.

The optimal clutter suppression performance that the system can theoretically achieve is to use the accurate clutter information actually contained in the CUT, namely, the accurate clutter covariance matrix $\mathbf{R}_c$ , to calculate the spatial-temporal two-dimensional adaptive weight $\mathbf{w}_{\mathrm{opt}}$ used by the array. Case 1 in Fig. 10 shows the MDV performance that the system can achieve in this case. Since the clutter information contained in the clutter covariance matrix is the most accurate, the position of the null in the MDV curve is the most accurate, and the

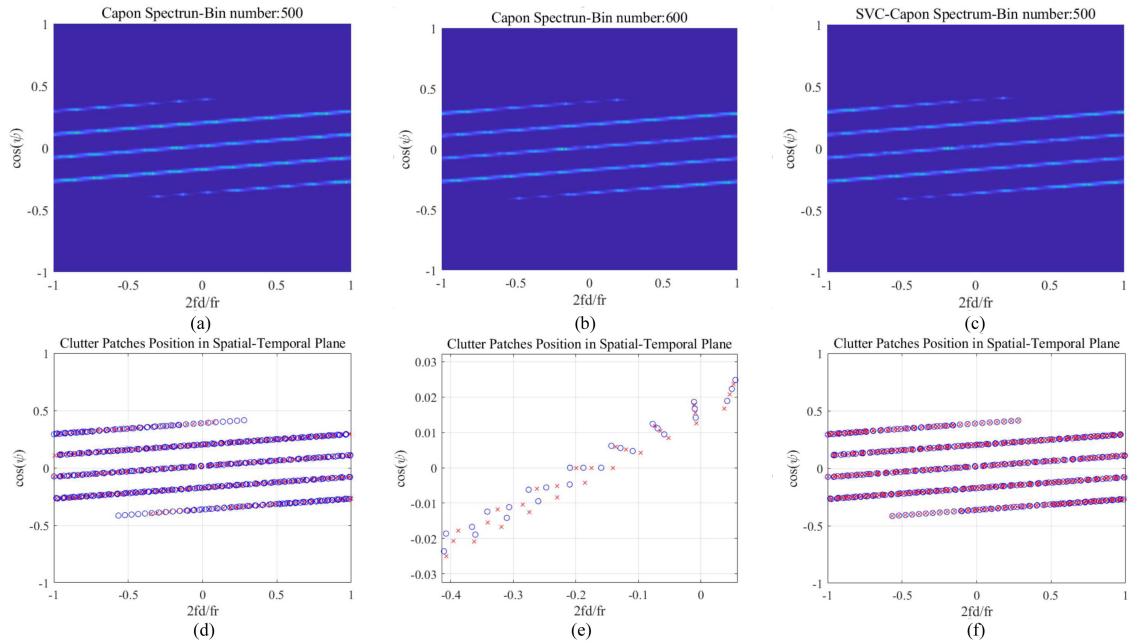


Fig. 7 Power spectrum of clutter and position distribution map of clutter patches. (a) Power spectrum of training sample numbered 500. (b) Power spectrum of CUT. (c) Power spectrum of corrected training sample. (d) Position information of clutter patches in training sample and CUT. (e) Position information of local clutter patches. (f) Position information of clutter patches in corrected training sample and CUT.

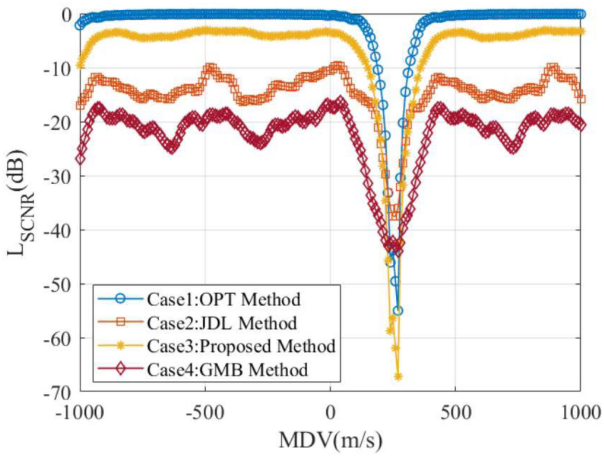


Fig. 8. MDV performance of system in simulated ground clutter environment.

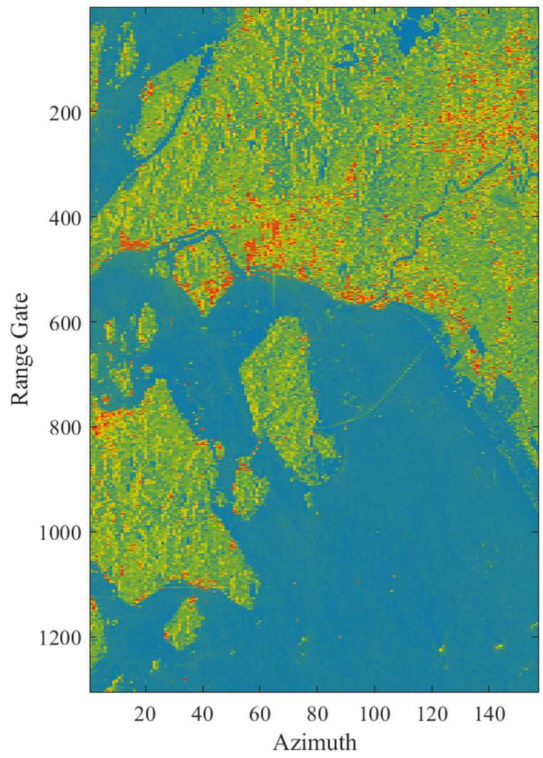


Fig. 9. Terrain map based on GF-3 satellite.

performance of clutter suppression that can be achieved is the optimal performance.

The traditional training sample selection methods, such as JDL-GIP, is used to select the training samples in the adjacent cells, and the clutter covariance matrix estimated by the clutter information of the training samples is $\hat{\mathbf{R}}_{n\_\mathrm{JDL}}$. Cases 2 and 4 in Fig. 10 show the MDV performance obtained by using the adaptive weight $\hat{\mathbf{w}}_{\mathrm{JDL}}$and $\hat{\mathbf{w}}_{\mathrm{GMB}}$. According to the simulation result in Cases 2 and 4, it can be found that the traditional method reduces the dimension of echo data by fixed dimension reduction structure, it cannot obtain all clutter information without considering the nonstationary nature of echo data itself. These factors lead to inaccurate clutter information contained in the reduced-order covariance matrix, and the estimated clutter energy is lower than the actual clutter energy. Compared with Case 2, although Case 4 can reduce the amount of computation, GMB method

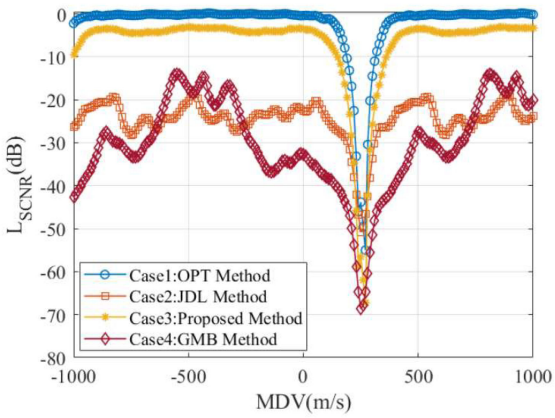


Fig. 10. MDV performance of system in simulated ground clutter environment.

selects fewer auxiliary channels, and nonstationary factors have a greater impact on this method. Finally, the output SCNR of the system is greatly reduced, the concave is widened and shallow, and the detection performance for slow-moving targets is also reduced. For the complex terrain at the land-sea interface, the clutter suppression performance obtained by the traditional method decreases more seriously.

In the simulation work of Case 3, we use the method proposed in this article to select all the adjacent cells that can be selected. First, the cells that are close to the amplitude distribution of the sample to be tested are selected as the training samples. Then, the spatial-temporal plane distribution position of the training samples is corrected by spatial variability. Finally, the covariance matrix of the training samples after sample correction is used to estimate the clutter covariance matrix of the unit to be tested, and the result is $\hat{\mathbf{R}}_{n\_\text{proposed}}$. In the area far from the main lobe clutter, the estimated clutter block power is higher than the actual value due to the channel synthesis of the receiving antenna and the use of space-time filter in the covariance matrix reconstruction. Compared with the results of the optimal processor, the SCNR loss of the system decreases by about 6 dB.

Through this method, we avoid the influence of spatial variability on the evaluation of sample similarity in traditional methods, and also avoid the performance loss caused by the spatial variability of clutter position information between training samples. According to the MDV performance curve of Case 3, it can be seen that the clutter suppression performance loss is much smaller than that of Cases 2 and 4, and the speed undetectable area is narrower, which is closer to the MDV performance that can be realized in the ideal situation. The proposed method realizes the accurate estimation of the clutter covariance matrix for SBEWR when the number of training samples is far from satisfying the R.M.B. criterion.

### C. Evaluation Index of MDV Performance

In the output power spectrum of SBEWR, the constant false alarm (CFAR) method is used to detect possible moving targets. According to the requirements of early warning tasks, the detection probability of the system is not less than 50%, and the false alarm probability is not more than $10^{-6}$. The output signal-to-clutter-noise ratio of the system should not be less than 12.63 dB to meet the detection requirements. Assuming that in the absence of clutter, the SNR that the system can provide is $a$ dB.

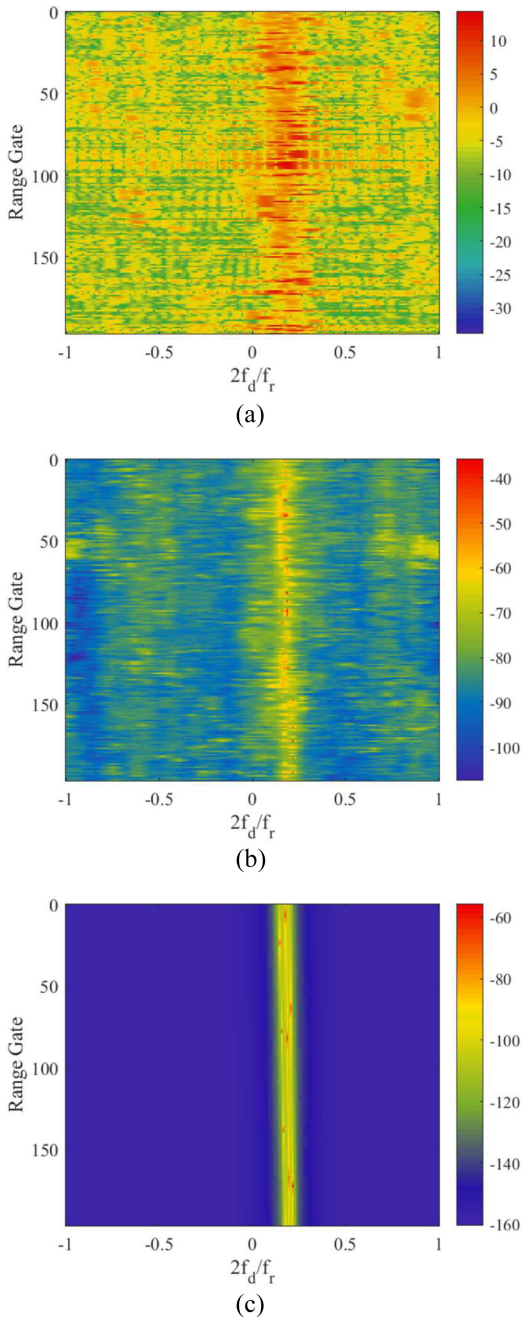


Fig. 11. Range–Doppler spectrum. (a) Range–Doppler spectrum of receive data. (b) Traditional method: JDL-GIP STAP method. (c) Proposed method: KLD + SVC method.

According to (18), the detected moving target area is shown in Fig. 10, and the output SCNR loss does not exceed $(a - 12.63)$ dB. Fig. 11 shows the Range–Doppler power spectrum of the received data of the range gate numbered 500–700. Fig. 11(a)

is the power spectrum of the original received data. Due to the nonstationary factors and heterogeneous environment, the clutter spectrum is seriously broadened and the overall power of the clutter is high. The system output power spectrum obtained by clutter suppression using the traditional method is shown in Fig. 11(b). Consistent with the previous analysis, due to the traditional method is not suitable for the clutter environment faced by SBEWR, the residual clutter power is high, and the clutter suppression is insufficient for the region far from the Doppler support area of the main lobe clutter. In Fig. 11(c), since the proposed method estimates the clutter covariance matrix of the CUT more accurately and suppresses the clutter more fully, the residual clutter power is lower than that of the traditional method, which greatly increases the detection ability of various types of targets.

For fast-moving targets with very small RCS, such as stealth aircraft, ballistic missiles, etc., the position in the power spectrum is generally far away from the main lobe clutter area. The proposed method can obtain smaller SCNR loss in the area away from the main lobe clutter, which can greatly improve the detection power of such targets. Since the SBEWR has the characteristics of long working distance, compared with AEWR, the echo energy of moving target is greatly reduced. The traditional method cannot obtain sufficient good clutter suppression performance in nonstationary and complex environments, and the output SCNR loss of the system is high, which makes it difficult to detect small and weak targets. Figs. 10 and 11 show that compared with the traditional method, the proposed method reduces the SCNR loss by about 15 dB and improves the detection distance by about 2.3 times. For large slow-moving targets near the main lobe clutter area, such as sea ships and airships, due to the narrower residual clutter width after suppression, the proposed method can obtain better MDV performance.

## V. Conclusion

In this article, a clutter covariance matrix estimation method for SBEWR is proposed. The proposed method focuses on decomposing the ground clutter information received by SBEWR into amplitude information and its position in the spatial-temporal plane. In the process of selecting training samples similar to the amplitude distribution of the CUT, the proposed method avoids the influence of spatial variability of clutter position information caused by nonstationary factors of SBEWR. Then, the space-time position information of the selected samples is corrected. The proposed method improves the estimation performance of clutter covariance matrix in the nonstationary and heterogeneous environment of SBEWR, and improves the clutter suppression performance. Experimental results verify the efficacy of the proposed method.

## References


[1] M. E. Davis, "Space based radar moving target detection challenges," in *Proc. RADAR*, 2002, pp. 143–147.

[2] P. A. Rosen and M. E. Davis, "A joint space-borne radar technology demonstration mission for NASA and the air force," in *Proc. IEEE Aerosp. Conf. Proc.*, vol. 1, 2003, pp. 1–444.

[3] M. Zhan, P. Huang, X. Liu, J. Chen, Y. Gao, and Z. Liu, "Performance analysis of space-borne early warning radar for AMTI," in *Proc. 6th Asia-Pacific Conf. Synthetic Aperture Radar*, 2019, pp. 1–6.

[4] J. Ai, Q. Luo, X. Yang, Z. Yin, and H. Xu, "Outliers-robust CFAR detector of Gaussian clutter based on the truncated-maximum-likelihood-estimator in SAR imagery.," *IEEE Trans. Intell. Transp. Syst.*, vol. 21, no. 5, pp. 2039–2049, May 2020.

[5] Jiaqiu Ai *et al.*, "Robust CFAR ship detector based on bilateral-trimmed-statistics of complex ocean scenes in SAR imagery: A closed-form solution.," *IEEE Trans. Aerosp. Electron. Syst.*, vol. 53, no. 3, pp. 1872–1890, Jun. 2021.

[6] J. Ai, X. Yang, J. Song, Z. Dong, L. Jia, and F. Zhou, "An adaptively truncated clutter-statistics-based two-parameter CFAR detector in SAR imagery.," *IEEE J. Ocean. Eng.*, vol. 43, no. 1, pp. 267–279, Jan. 2017.

[7] Ding Tao, S. N. Anfinsen, and C. Brekke, "Robust CFAR detector based on truncated statistics in multiple-target situations.," *IEEE Trans. Geosci. Remote Sens.*, vol. 54, no. 1, pp. 117–134, Jan. 2016.

[8] M. Rangaswamy, "An overview of space-time adaptive processing for radar," in *Proc. Int. Conf. Radar*, 2003, pp. 45–50.

[9] L. B. Fertig, "Analytical expressions for space-time adaptive processing (STAP) performance," *IEEE Trans. Aerosp. Electron. Syst.*, vol. 51, no. 1, pp. 42–53, Jan. 2015.

[10] W. L. Melvin, "Space-time adaptive radar performance in heterogeneous clutter," *IEEE Trans. Aerosp. Electron. Syst.*, vol. 36, no. 2, pp. 621–633, Apr. 2000.

[11] W. L. Melvin, "A STAP overview," *IEEE Aerosp. Electron. Syst. Mag.*, vol. 19, no. 1, pp. 19–35, Jan. 2004.

[12] I. D. Reed, J. D. Mallett, and L. E. Brennan, "Rapid convergence rate in adaptive arrays," *IEEE Trans. Aerosp. Electron. Syst.*, vol. 10, no. 6, pp. 853–863, Nov. 1974.

[13] I. S. Reed, J. D. Mallett, and L. E. Brennan, "Rapid convergence rate in adaptive arrays," *IEEE Trans. Aerosp. Electron. Syst.*, vol. AES-10, no. 6, pp. 853–863, Nov. 1974.

[14] S. Mangiat, K. Y. Li, S. Unnikrishna Pillai, and B. Himed, "Effect of terrain modeling and internal clutter motion on space based radar performance," in *Proc. IEEE Conf. Radar*, 2006, pp. 310–317.

[15] J. Maher, M. Callahan, and D. Lynch, "Effects of clutter modeling in evaluating STAP processing for space-based radars," in *Proc. Rec. IEEE 2000 Int. Radar Conf.*, 2000, pp. 565–570.

[16] S. U. Pillai, B. Himed, and Ke Yong Li, "Modeling of earth's rotation for space based radar," in *Proc. Conf. Rec. Thirty-Eighth Asilomar Conf. Signals, Syst. Comput.* vol. 2, 2004, pp. 1682–1686.

[17] S. Pillai, B. Himed, and K. Y. Li, "Effect of earth's rotation and range foldover on space-based radar performance," *IEEE Trans. Aerosp. Electron. Syst.*, vol. 42, no. 3, pp. 917–932, Jul. 2006.

[18] J. S. Bird and A. W. Bridgewater, "Performance of space-based radar in the presence of earth clutter," *IEE Proc. F-Commun., Radar Signal Process.*, vol. 131, no. 2, pp. 491–500, 2008.

[19] Y. L. Wang, J. W. Chen, B. Zheng, and Ying-Ning Peng, "Robust space-time adaptive processing for airborne radar in nonhomogeneous clutter environments," *IEEE Trans. Aerosp. Electron. Syst.*, vol. 39, no. 1, pp. 70–81, Jan. 2003.

[20] Z. Xin, Q. Yang, and W. Deng, "Weak target detection within the nonhomogeneous ionospheric clutter background of HFSWR based on STAP," *Int. J. Antennas Propag.*, vol. 2013, no. 6, pp. 1212–1215, 2013.

[21] X. Yang, Y. Liu, and T. Long, "Robust non-homogeneity detection algorithm based on prolate spheroidal wave functions for space-time adaptive processing," *IET Radar, Sonar; Navigation*, vol. 7, no. 1, pp. 47–54, 2013.

[22] Y. Wu, T. Wang, J. Wu, and J. Duan, "Training sample selection for space-time adaptive processing in heterogeneous environments," *IEEE Geosci. Remote Sens. Lett.*, vol. 12, no. 4, pp. 691–695, Apr. 2015.

[23] B. Tang, J. Tang, and Y. Peng, "Detection of heterogeneous samples based on loaded generalized inner product method," *Digit. Signal Process.*, vol. 22, no. 4, pp. 605–613, Jul. 2012.

[24] M. Rangaswamy, P. Chen, J. H. Michels, and B. Himed, "A comparison of two non-homogeneity detection methods for space-time adaptive processing," in *Proc. IEEE Sensor Array Multichannel Signal Process. Workshop Proc.*, 2002, pp. 355–359.

[25] D. J. Rabideau and A. Steinhardt, "Improved adaptive clutter cancellation through data-adaptive training," *IEEE Trans. Aerosp. Electron. Syst*, vol. 35, no. 3, pp. 879–891, Jun. 1999.

[26] M. C. Wicks, M. Rangaswamy, R. Adve, and T. B. Hale, "Space-time adaptive processing: A knowledge-based perspective for airborne radar," *IEEE Signal Process. Mag.*, vol. 23, no. 1, pp. 51–65, Jan. 2006.
[27] J. R. Guerci and E. J. Baranoski, "Knowledge-aided adaptive radar at DARPA: An overview," *IEEE Signal Process. Mag.*, vol. 23, no. 1, pp. 41–50, Jan. 2006.
[28] J. Ward, "Space-time adaptive processing for airborne radar," in *Proc. Int. Conf. Acoust., Speech, Signal Process.*, vol. 5, 1995, pp. 2809–2812.
[29] R. Klemm, "Adaptive clutter suppression for airborne phased array radars," *Commun., Radar Signal Process., IEE Proc. F*, vol. 130, no. 1, pp. 125–132, 1983.
[30] L. E. Brennan and F. M. Staudaher, "Sub-clutter visibility demonstration," Adaptive Sensors Incorporated, Santa Monica, CA, USA, Technical Report RL-TR-98-91, Mar. 1992.
[31] X. Hua, Y. Cheng, H. Wang, Y. Qin, and Y. Li, "Geometric means and medians with applications to target detection," *IET Signal Process.*, vol. 11, no. 6, pp. 711–720, Aug. 2017.
[32] X. Hua, Y. Cheng, H. Wang, Y. Qin, Y. Li, and W. Zhang, "Matrix CFAR detectors based on symmetrized Kullback–Leibler and total Kullback–Leibler divergences," *Digit. Signal Process.*, vol. 69, pp. 106–116, Oct. 2017.
[33] B. C. Vemuri, M. Liu, S.-I. Amari, and F. Nielsen, "Total Bregman divergence and its applications to DTI analysis," *IEEE Trans. Med. Imag.*, vol. 30, no. 2, pp. 475–483, Feb. 2011.
[34] F. D. Lapierre, M. Van Droogenbroeck, and J. G. Verly, "New methods for handling the range dependence of the clutter spectrum in non-sidelooking monostatic STAP radars," in *Proc. IEEE Int. Conf. Acoust., Speech, Signal Process., Proc.*, 2003, pp. 5–73.
[35] J. A. Ziegler, R. E. Ziemer, and R. P. Breuggemann, "A simple comprehensive clutter model for evaluation of pulse Doppler radar," in *Proc. Nat. Electron. Conf.*, 1973, pp. 144–150.

**Tianfu Zhang** (Student Member, IEEE) was born in Tangshan, Hebei, China, in 1996. He received the B.S. degree in electronic science and technology from Xidian University, Xi'an, China, in 2018, where he is currently working toward the Ph.D. degree in signal processing with the National Laboratory of Radar Signal Processing.

His research interests include space-based early warning radar system design and signal processing method.

**Zhihao Wang** (Student Member, IEEE) was born in Anhui, China, in 1995. He received the B.S. degree in electronic information engineering from Xidian University, Xi'an, China, in 2017, where he is currently working toward the Ph.D. degree in signal processing with the National Laboratory of Radar Signal Processing.

His research interests include synthetic aperture radar ground moving target indication (SAR-GMTI), spaceborne early warning radar system design, and signal processing method.

**Ning Qiao** was born in Henan, China, in 1997. She received the B.S. degree in communication engineering from Northwestern Polytechnical University, Xi'an, China, in 2020, where she is currently working toward the Ph.D. degree with electronic science and technology.

Her research interests include space time adaptive signal processing and space based early warning radar.

**Shuangxi Zhang** (Member, IEEE) was born in Fujian, China, in 1984. He received the B.S. degree in the technique of measuring control and instrument engineering from Xidian University, Xi'an, China, in 2008, and the Ph.D. degree in signal processing from the National Key Laboratory of Radar Signal Processing, Xidian University, in 2014.

He was a Research Fellow with the National University of Singapore (NUS), Singapore from 2014 to 2016. He is an Associate Professor with the School of Electronics and Information, Northwestern Polytechnical University, Xi'an, China. He is also the Organizer and the Session Chairs of Synthetic Aperture Radar Techniques and Applications-Part1/2 and -Part2/2 in ACES-China 2017, Suzhou, China. His research interests include SAR imaging, clutter suppression, SAR interference suppression, array signal processing, electromagnetic scattering, etc.

**Mengdao Xing** (Fellow, IEEE) received the B.S. and Ph.D. degrees in electronic engineering from Xidian University, Xi'an, Shaanxi, China, in 1997 and 2002, respectively.

He is a Professor with the National Laboratory of Radar Signal Processing, Xidian University. He is the Dean with the Academy of Advanced Interdisciplinary Research Department, Xidian University. He has authored or coauthored more than 200 refereed scientific journal articles. He has also authored or coauthored two books about SAR signal processing. He holds more than 50 authorized Chinese patents. His research interests include synthetic aperture radar (SAR), SAR interferometry (InSAR), inversed SAR (ISAR), sparse signal processing, and microwave remote sensing.

Dr. Xing has held several Special Issues on IEEE GRSM and JSTARS. He is the Associate Editor for Radar Remote Sensing of the IEEE TRANSACTIONS ON GEOSCIENCE AND REMOTE SENSING and the Editor-in-Chief for the MDPI Sensors. The total citation times of his research are greater than 10 000 (H-index 50). He was rated as the Most Cited Chinese Researcher by Elsevier. His research has been supported by various funding programs, such as National Science Fund for Distinguished Young Scholars.

**Yongliang Wang** received the Ph.D. degree in electrical engineering from Xidian University, Xi'an, China, in 1994.

From 1994 to 1996, he was a Postdoctoral Fellow with the Department of Electronic Engineering, Tsinghua University, Beijing, China. He has been a Full Professor since 1996, and was the Director with the Key Research Laboratory, Wuhan Radar Academy, Wuhan, China, from 1997 to 2005. He has authored or coauthored three books and more than 200 papers. His research interests include radar systems, space–time adaptive processing, and array signal processing.

Dr. Wang is a Member of the Chinese Academy of Sciences and a Fellow of the Chinese Institute of Electronics. He was a recipient of the China Postdoctoral Award in 2001 and the Outstanding Young Teachers Award of the Ministry of Education, China, in 2001.